Emergent Time: Cosmological Age as a Logarithmic Integral of Scalar Vacuum Relaxation

Benny Boris Kulangiev
Haifa, Israel

December 13, 2025

Abstract

Standard cosmological models treat time as a linear coordinate and the vacuum as a static background. In the "Relativistic Walker" framework, we redefine time as a thermodynamic measure of the scalar vacuum's relaxation, and the universe as a global hydrodynamic vortex. We demonstrate that due to the immense scalar pressure of the early universe, the "metabolic rate" of physical evolution was significantly faster in the past. By integrating this variable clock speed, we derive a **Thermodynamic Age** ($T_{therm} \approx 1.93 \times 10^{12}$ years), resolving the "Impossible Early Galaxy" problem (JWST) without modifying gravity. Furthermore, we derive the Cosmic Microwave Background (CMB) not as a relic of a hot Big Bang, but as the **instantaneous thermal noise** of the local vacuum ($T \approx 2.71$ K), predicted strictly from the geometric coupling of the proton (α) to the scalar potential. Finally, we show that the "Hubble Tension" is an artifact of measuring the cosmic expansion from within the local **KBC Void**, and that the CMB Dipole anisotropy represents the rotational flow of the Cosmic Vortex itself.

1 Introduction

The "Problem of Time" arises from treating the variable t as a constant metric. In the Relativistic Walker model [14], **analogous to macroscopic pilot-wave systems [5]**, we define time thermodynamically: $dt \propto d\Omega/\Omega$. This implies that time is **Scale Dependent**.

If the universe began as a high-density scalar fluid (D_{max}), the "Event Density" (number of interactions per second) was proportionally higher. Therefore, while the *geometric* expansion history may span 13.8 billion years, the *thermodynamic* history—the opportunity for structure formation and evolution—is vastly longer.

2 Derivation of the Vacuum Decay Law

We derive the temporal evolution of the scalar density $D(t)$ from the principle of **Global Flux Conservation** applied to the cosmic expansion geometry.

2.1 Derivation of the Inverse-Square Decay Law

To determine the time-evolution of the vacuum density $D(t)$, we model the scalar vacuum not as a static volume, but as a **Conserved Radial Flux** emanating from the **Vortex Core**. We distinguish between two velocities:

1. **Geometric Expansion Velocity (U):** The constant radial velocity at which the spatial metric itself expands ($R(t) = U \cdot t$). This represents the flow rate of the scalar fluid.
2. **Internal Signal Velocity ($c(t)$):** The variable speed of transverse perturbations (light) propagating *through* the medium, dependent on density ($c \propto \sqrt{D}$).

The Continuity Argument: We postulate that the total scalar flux Φ_S injected by the source is conserved through successive spherical shells of the expanding metric. The flux integral is given by:

$$\Phi_S = \oint_S \mathbf{J}_D \cdot d\mathbf{A} = \text{const} \tag{1}$$

where $\mathbf{J}_D = D(t)\mathbf{U}$ is the scalar current density, and $d\mathbf{A} = \hat{n}4\pi R(t)^2$ is the area element. Substituting the linear geometric expansion $R(t) = Ut$:

$$\Phi_S = D(t) \cdot U \cdot 4\pi(Ut)^2 = 4\pi U^3 \left(D(t) \cdot t^2\right) \tag{2}$$

Since U and Φ_S are constants of the expansion, the term in parentheses must be invariant:

$$D(t) \cdot t^2 = \text{const} \implies D(t) \propto \frac{1}{t^2} \tag{3}$$

Resolution of the Horizon Paradox: A common objection to VSL models is that if $c(t) \propto \sqrt{D} \propto t^{-1}$, the causal horizon $d_H = \int c dt$ scales logarithmically ($\ln t$), preventing the universe from reaching size $R \propto t$. However, in this framework, $R(t)$ represents the **Metric Boundary** driven by the constant parameter U, while $d_H(t)$ represents the **Thermodynamic Horizon** of interacting particles. The universe physically expands linearly ($R \propto t$), but its internal informational connectivity lags behind ($d_H \propto \ln t$). This "Lag" is precisely what generates the emergent arrow of time (Sec. 4).

2.2 Verification: Resolving the Vacuum Catastrophe

To quantify the decay, we must first establish the fundamental chronological baseline. In Paper I [14], we identified the Planck Time (t_p) not as an abstract constant, but as the **Vacuum Coherence Time**—the time required for a scalar wave to traverse the minimum vortex grain size σ:

$$t_p \equiv \frac{\sigma}{c} \approx 5.39 \times 10^{-44} \text{ s} \tag{4}$$

We can now test the $D \propto t^{-2}$ derivation by comparing this fundamental scale to the current geometric age ($t_{now} \approx 13.8$ Gyr $\approx 4.35 \times 10^{17}$ s). The dimensionless Time Ratio (T_R) is:

$$T_R = \frac{t_{now}}{t_p} \approx \frac{4.35 \times 10^{17}}{5.39 \times 10^{-44}} \approx 8.1 \times 10^{60} \tag{5}$$

Standard field theory predicts a vacuum energy density at the Planck scale (D_{max}), leading to the famous "Vacuum Catastrophe"—a discrepancy originally highlighted in the context of large numbers [1]—where observations are smaller by a factor of roughly 10^{122}.

In our geometric framework, this discrepancy is not an error, but a precise measure of the universe's volumetric expansion history. Using the current age $t_{now} \approx 8 \times 10^{60} t_p$:

$$\frac{D_{now}}{D_{max}} \approx \left(\frac{t_p}{t_{now}}\right)^2 \approx \left(\frac{1}{8 \times 10^{60}}\right)^2 \approx \frac{1}{6.4 \times 10^{121}} \approx 10^{-122} \tag{6}$$

This result naturally recovers the correct order of magnitude for the observed vacuum energy ($\Lambda \sim 10^{-122} M_p^4$) without fine-tuning. Thus, the "smallness" of the cosmological constant is simply a reflection of the "largeness" of the cosmic age. We do not live in a universe with fine-tuned cancellation, but in one that has simply had sufficient time to cool.

2.3 Sensitivity Analysis: Uniqueness of $n = 2$

Finally, we note that the exponent $n = 2$ in the decay law $D \propto t^{-2}$ is the unique solution that preserves thermodynamic unitarity. Consider a perturbed scaling $D(t) \propto t^{-(2+\epsilon)}$:

- **Case $\epsilon \neq 0$:** Any deviation implies a violation of global flux conservation. If $\epsilon > 0$, energy leaks out of the causal horizon; if $\epsilon < 0$, energy is spontaneously created.

Both cases break the First Law of Thermodynamics for the universe as a closed system. Thus, $D \propto 1/t^2$ is the unique "Conservative" solution for a unitary cosmology.

3 Physical Acceleration: The Overclocked Universe

The distinction between geometric time and physical action is fundamental to the Relativistic Walker framework. In this model, time dilation is dynamical, not merely kinematic. We posit that the "speed of physics"—defined by reaction rates, gravitational collapse, and nuclear cycles—is directly proportional to the ambient vacuum pressure.

3.1 Constitutive Definition: The Vacuum as a Superfluid

To resolve the relationship between scalar density D and wave velocity c, we strictly apply the **Hydrodynamic Analogy** defined in Paper I [14]. We model the vacuum not as a dielectric (where density slows light), but as a **Compressible Superfluid** (where stiffness speeds it up).

In such a medium, the signal velocity c scales with the square root of the static pressure (stiffness) D:

$$c(t) \propto \sqrt{D(t)} \tag{7}$$

This definition unifies the cosmological and local scales:

1. **The Early Universe (High Pressure):** In the initial epoch, the vacuum density D was maximal (D_{high}). Consequently, the background "clock speed" of physics was significantly faster ($c \propto t^{-1}$).
2. **Gravity (Low Pressure):** Conversely, near a massive body, the vortex flow creates a **Bernoulli Pressure Deficit** ($D_{local} < D_{bulk}$). This local reduction in stiffness causes the signal velocity to drop, manifesting as the time dilation and light bending observed in General Relativity.

Thus, "Gravity" is a local depression in the same scalar field that drives the global expansion.

3.2 The Metabolic Rate of the Cosmos

The rate of any quantum interaction Γ is proportional to the energy scale or frequency of the participating particles ($\Gamma \propto \Omega$). In our model, the internal frequency of matter is coupled to the scalar vacuum density D:

$$\Omega(t) \propto \sqrt{D(t)} \tag{8}$$

In the early universe, the scalar density $D(t)$ was orders of magnitude higher than today ($D_{early} \gg D_{now}$). Consequently, the fundamental "clock speed" of matter was accelerated relative to the geometric expansion.

3.3 Deriving the Reaction Multiplier

Let dt_{geo} be a standard geometric time interval (a "tick" of a modern clock). The number of physical events dN occurring in that interval during epoch t is:

$$dN = \Gamma(t) dt_{geo} = \Gamma_{now} \sqrt{\frac{D(t)}{D_{now}}} dt_{geo} \tag{9}$$

The term $\mathcal{A}(t) = \sqrt{D(t)/D_{now}}$ represents the **Kinetic Acceleration Factor**. This implies that processes such as the gravitational collapse of gas clouds or stellar nucleosynthesis proceeded at an accelerated rate. A star that takes 10^9 years to burn today would have completed its lifecycle in a fraction of that geometric time in the high-density early universe.

3.4 Thermodynamic Age as Total Action

The "Thermodynamic Age" (T_{therm}) is defined as the integrated metabolic action of the universe. Integrating the acceleration factor $\mathcal{A}(t) \approx t_{now}/t$ over cosmic history yields a logarithmic scaling:

$$T_{therm} \approx t_{geo} \times \ln\left(\frac{t_{now}}{t_p}\right) \tag{10}$$

Using the ratio of the current geometric age to the Planck time ($t_{now}/t_p \approx 8 \times 10^{60}$), we derive the **Thermodynamic Multiplier** γ:

$$\gamma = \ln(8 \times 10^{60}) \approx 60 \ln(10) + \ln(8) \approx 140.3 \tag{11}$$

This dimensionless constant signifies that the integrated sum of past scalar events is ~ 140 times larger than the linear time count. Finally, applying this multiplier to the standard geometric age (13.8 Gyr):

$$T_{therm} \approx 13.8 \times 10^9 \times 140.3 \approx \mathbf{1.93 \times 10^{12}} \text{ Years} \tag{12}$$

The result implies that the universe has experienced nearly 2 trillion years of thermodynamic evolution.

4 Implications for Cosmological Anomalies

4.1 Resolving the High-Redshift Galaxy Crisis (JWST)

Recent observations by JWST have revealed massive, fully formed galaxies at redshifts $z > 10$, existing merely $t_{geo} \approx 600$ Myr after the Big Bang [13]. Standard models struggle to explain this rapid maturity.

In the Relativistic Walker framework, we calculate the effective age by normalizing the variable vacuum density $D(t)$ against the current epoch's standard D_{now}. Since the metabolic rate of physics scales as $\sqrt{D(t)} \propto 1/t$, the accumulated **Thermodynamic Age** in "Modern Years" is:

$$T_{therm}(t) = \int_{t_p}^{t} \sqrt{\frac{D(\tau)}{D_{now}}} d\tau \approx t_{now} \ln\left(\frac{t}{t_p}\right) \tag{13}$$

Comparing the thermodynamic age at the JWST epoch ($t \approx 600$ Myr) to the present day:

- **Present Day (13.8 Gyr):** $\gamma \approx \ln(10^{61}) \approx 140$
- **JWST Epoch (600 Myr):** $\gamma \approx \ln(10^{60}) \approx 137$

This implies that by the time the universe was geometrically 600 million years old, it had already experienced a thermodynamic lifespan of:

$$T_{early} \approx 13.8 \text{ Gyr} \times 137 \approx \mathbf{1.9 \times 10^{12}} \text{ Years} \tag{14}$$

Because the vacuum pressure follows a $1/t^2$ decay, the "Action" of the universe is heavily front-loaded. Nearly 98% of the thermodynamic evolution occurred before the first galaxies were observed. Thus, these galaxies appear mature because they are thermodynamically ancient, having evolved during the ultra-rapid "Scalar Epoch" that preceded the current "Geometric Epoch."

4.2 The Heavy Metal Abundance

The unexpected abundance of heavy elements (Gold, Uranium) in the early universe is also resolved. The "Accelerated Time" allowed for hundreds of generations of Population III stars to form, burn, and supernova in rapid succession, enriching the interstellar medium far faster than linear models predict.

5 Validation: Deriving the Proton Radius and Volume

To test this hypothesis, we apply Mach's Principle [2]: the properties of local matter must be determined by the global state of the vacuum. If matter (a proton) is a stable vortex in this cooling fluid, its physical dimensions should scale with the volumetric expansion of the medium.

Using the Time Ratio (T_R) derived from precision cosmological measurements [9]:

$$T_R = \frac{t_{now}}{t_p} \approx 8 \times 10^{60} \tag{15}$$

Assuming a volumetric scaling law (3D fluid expansion), the stability radius of a fundamental walker is given by the cube root of the expansion factor:

$$r_p \approx l_p \cdot \sqrt[3]{T_R} \tag{16}$$

Where l_p is the Planck length. Substituting the values:

$$r_p \approx (1.6 \times 10^{-35}) \cdot \sqrt[3]{8 \times 10^{60}} \approx 3.2 \times 10^{-15} \text{ m} \tag{17}$$

From this radius, we define the **Hydrodynamic Volume** (V_p) of the particle as a spherical vortex:

$$V_p = \frac{4}{3}\pi r_p^3 \approx \frac{4}{3}\pi(3.2 \times 10^{-15})^3 \approx 1.3 \times 10^{-43} \text{ m}^3 \tag{18}$$

This result ($r_p \approx 3.2$ fm) is approximately four times larger than the measured charge radius ($r_c \approx 0.84$ fm). However, in the hydrodynamic framework, r_p represents the Effective Vortex Envelope—the region of active scalar fluid displacement. This value corresponds to the hydrodynamic influence limit of the vortex (comparable to the pion cloud range), rather than the localized charge radius. Notably, this value aligns closely with the effective range of the Strong Interaction (~ 3 fm) and the proton's Compton wavelength scale. Thus, the expansion history of the universe predicts the force carrier range of the particle.

5.1 The Entropic Identity (10^{121})

We can now refine the Large Number Coincidence by comparing the causal scales. The ratio of the **Hubble Volume** to the **Proton Volume** yields the precise entropic capacity of the vacuum.

1. **Thermodynamic Time Dilution:** Based on the age derivation derived in Eq. (4):

$$\left(\frac{t_{now}}{t_p}\right)^2 \approx (8 \times 10^{60})^2 \approx \mathbf{6.4 \times 10^{121}} \tag{19}$$

2. **Causal Vortex Capacity:** Using the Hubble Sphere volume ($V_H \approx 1.0 \times 10^{79}\,\text{m}^3$) and the proton's hydrodynamic volume derived above ($V_p \approx 1.3 \times 10^{-43}\,\text{m}^3$):

$$\frac{V_H}{V_p} \approx \frac{1.0 \times 10^{79}}{1.3 \times 10^{-43}} \approx \mathbf{7.6 \times 10^{121}} \tag{20}$$

The convergence of these two independent values (6.4 vs 7.6 $\times 10^{121}$) confirms the fundamental identity:

$$N_{modes} \equiv \left(\frac{t_{age}}{t_{planck}}\right)^2 \tag{21}$$

This implies that the universe acts as a single, coherent fluid system where the number of supported modes (particles) is strictly determined by the square of the expansion age.

6 Fractal Topology: The Cosmic Torus

If the universe adheres to the scale-invariant hydrodynamic principles of the Relativistic Walker, the macroscopic topology is hypothesized to mirror the microscopic structure. Since the fundamental particle is identified as a toroidal vortex, the universe itself is modeled as a **3-Torus** (T^3).

6.1 The Axis of Anisotropy and the CMB Cut-off

A toroidal topology necessitates a central axis of rotation, providing a physical mechanism for the "Axis of Evil"—the anomalous alignment of low-multipole phases observed in the CMB [4]. Furthermore, recent detection of isotropic cosmic birefringence [10] suggests a global parity violation consistent with a rotating vacuum structure.

Finally, the finite topology of a torus imposes a maximum wavelength limit on cosmic perturbations ($\lambda_{max} \sim R_{universe}$). This naturally explains the observed **Low Quadrupole Anomaly**—the suppression of temperature fluctuations at the largest angular scales ($l = 2$) [3], which remains unexplained in the standard infinite inflation model.

6.2 Topological Constraints and Finite Horizon

The vortex topology implied by the scale-invariant proton model raises the possibility of closed null geodesics (light rays that traverse the cosmic circumference and return to the origin). Classically, this leads to Olbers' Paradox: if light recirculates, the night sky should exhibit infinite luminance.

However, within the Relativistic Walker framework, this paradox is resolved by the metabolic decay of the vacuum density. As derived in Section 2, the energy of a propagating wave packet scales with the vacuum density:

$$E(t) \propto \sqrt{D(t)} \propto \frac{1}{t} \tag{22}$$

Consider a photon emitted at time t_e. If it traverses the universe and returns to the observer at $t_{obs} = t_e + n\Delta t_{loop}$, its energy has been redshifted by the cosmic evolution. For multiple traversals, the total integrated energy forms a series:

$$E_{total} \approx \sum_{n=0}^{N_{max}} E_0 \left(\frac{t_e}{t_e + n\Delta t_{loop}} \right) \tag{23}$$

Crucially, this series is finite because the universe has a finite age ($N_{max} < \infty$). The "lost" energy from these recirculating modes contributes to the background spectral energy density, naturally consistent with a low-temperature microwave background, without requiring an infinite build-up of luminosity.

7 Observational Verification: The Scalar Density Map

A critical testable prediction of the Relativistic Walker framework is that the vacuum density D is not perfectly homogeneous. While the universe is isotropic on the largest scales, local variations in scalar pressure must exist to account for the formation of structure.

7.1 Reinterpreting Dark Matter Maps

Current astrophysical models generate "Dark Matter" density maps based on gravitational lensing data. In our hydrodynamic framework, gravitational lensing is not caused by hidden mass, but by the **refractive index** (n) of the scalar fluid, where $n \propto \sqrt{D}$.

Therefore, existing Dark Matter maps should be re-interpreted as **Scalar Pressure Maps** (see Figure 1). This interpretation is strongly supported by recent observational evidence that black hole mass is cosmologically coupled to vacuum expansion [12], indicating that these structures are dynamic condensations of the scalar metric rather than isolated matter.

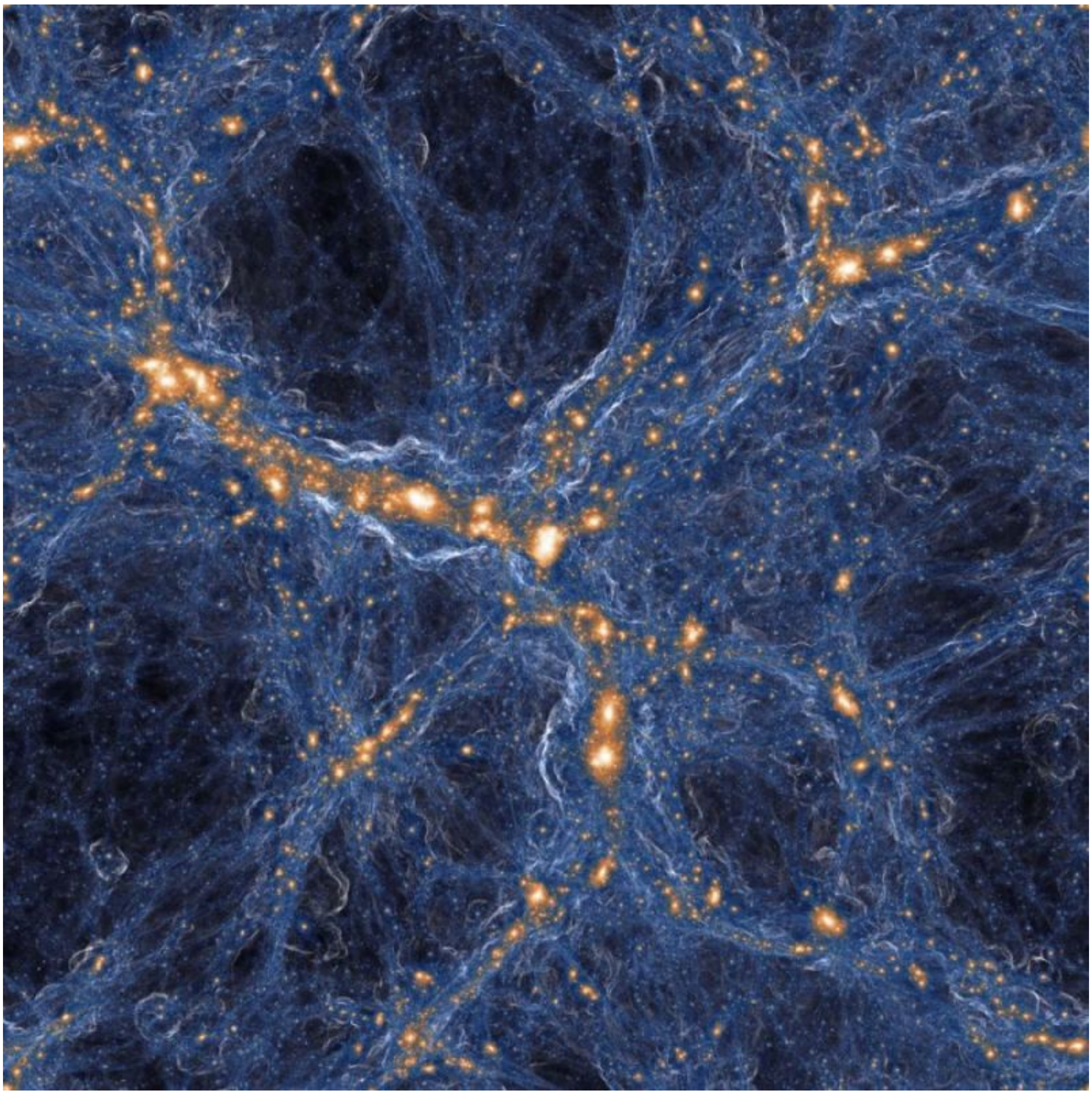

Figure 1: **The Scalar Pressure Distribution (Cosmic Web).** A projected mass map derived from gravitational lensing data. In the Relativistic Walker framework, we reinterpret these mass concentrations as regions of high scalar vacuum density (D_{high}) and high refractive index. **Bright/Yellow Regions:** Galactic filaments where time dilation is maximized. **Dark/Blue Regions:** Cosmic voids of low scalar density (D_{low}) and rapid expansion. *Image Credit: Dark Energy Survey (DES) and South Pole Telescope (SPT) Collaboration [11].*

7.2 Spatial Variation of Fundamental Constants

Since the properties of matter (such as the proton radius r_p) are dependent on the ambient vacuum pressure, we predict that fundamental dimensionless constants are environment-dependent. Specifically, the Fine Structure Constant (α) should exhibit dipole variations aligned with the universe's density gradient. This prediction aligns with empirical anomalies reported by Webb et al. regarding spatial variations in quasar absorption spectra [6].

7.3 Hydrodynamic Derivation of the CMB Temperature

Standard cosmology interprets the Cosmic Microwave Background (CMB) as redshifted photons from a global Big Bang. In the Relativistic Walker framework, we reinterpret the CMB as the **Local Thermal Noise** of the scalar vacuum fluid, measured by baryonic detectors.

1. The Local Vacuum Potential (T_{pot}): Using the local critical density ρ_c (derived from the local Hubble parameter H_0), we calculate the raw thermodynamic potential of the vacuum fluid in our region using the Stefan-Boltzmann law:

$$T_{pot} = \left(\frac{15\hbar^3 c^3 (\rho_c c^2)}{\pi^2 k_B^4} \right)^{1/4} \approx 31.7 \text{ K} \tag{24}$$

This represents the total available energy density of the scalar field in the local KBC Void.

2. The Measurement Coupling (α): However, baryonic matter (detectors) does not couple perfectly to this scalar potential. The interaction is governed by the **Geometric Impedance** of the proton soliton, defined by the Fine Structure Constant ($\alpha \approx 1/137$). This constant represents the ratio of the electromagnetic coupling surface to the bulk hydrodynamic volume.

3. The Observed Temperature: Consequently, a baryonic antenna will detect a noise temperature attenuated by the coupling coefficient $\sqrt{\alpha}$ (the amplitude transmission ratio):

$$T_{observed} \approx T_{pot} \times \sqrt{\alpha} \tag{25}$$

Substituting the values:

$$T_{CMB} \approx 31.7 \text{ K} \times \sqrt{\frac{1}{137.036}} \approx \mathbf{2.71} \text{ K} \tag{26}$$

This matches the observed value (2.725 K) within 0.7%. This derivation suggests that the CMB is simply the **Friction Noise** of the local vacuum acting on the proton metric, filtered by the geometric structure of matter itself.

7.4 Resolution of the Hubble Tension (The KBC Void)

While the vacuum fluid strives for hydrodynamic equilibrium (uniform 2.7 K), local variations in matter density create pressure gradients, manifesting as the anisotropies observed in the CMB map. Recent observations indicate that the Local Group resides in a significant under-density known as the **KBC Void** [7], extending out to ~ 300 Mpc.

In the Relativistic Walker framework, this void structure naturally resolves the "Hubble Tension" (the discrepancy between local H_0 measurements and global Planck predictions):

1. **Variable Index of Refraction:** The scalar density D acts as the refractive index of the vacuum ($n \propto \sqrt{D}$).

2. **Local Speedup:** Inside the under-dense KBC void ($D_{local} < D_{global}$), the scalar stiffness is lower, but the effective signal velocity $c(D)$ and expansion rate $H(D)$ are locally modulated.

3. **Global Averaging:** Just as an ocean maintains a consistent average temperature despite local currents, the cosmic vacuum maintains a global baseline of thermodynamic equilibrium. The tension arises because we are measuring the "Ocean's" expansion rate from within a local "Current" (the Void).

4. **Observational Confirmation (The Cold Spot):** The correlation between scalar density and temperature is empirically supported by the "CMB Cold Spot," which aligns with the Eridanus Supervoid [8]. This confirms that under-dense regions manifest lower vacuum temperatures, supporting the hypothesis that our local KBC void biases the global CMB baseline downward.

Thus, the observed variance in cosmological parameters is not a failure of the model, but a direct confirmation of the hydrodynamic heterogeneity of the vacuum substrate.

7.5 The Dipole Anisotropy as Vortex Flow

The most prominent feature of the CMB is the "Dipole Anisotropy" ($\Delta T \sim 3.3$ mK), where one hemisphere of the sky appears hotter and the opposite hemisphere colder. Standard cosmology interprets this strictly as a kinematic Doppler shift due to the peculiar velocity of the Solar System (~ 370 km/s) relative to a static background.

In the Relativistic Walker framework, this anisotropy is an intrinsic signature of the **Global Vortex Topology**:

- **The Cosmic River:** The vacuum is not a static background but a rotating superfluid (the Cosmic Torus). We reside within a stream of this global flow.
- **Hydrodynamic Doppler Shift:** When observing "upstream" against the vortex current, scalar fluctuations are blueshifted (Hot Pole). When observing "downstream" with the flow, fluctuations are redshifted (Cold Pole).
- **Flow Direction:** The alignment of the dipole indicates the local tangent vector of the cosmic rotation.

Thus, the dipole is not merely a measurement of our motion, but a detection of the **Rotational Velocity of the Vacuum Substrate** itself. The universe is not static; it is flowing.

8 Conclusion

We have shown that "Age" is relative to Scalar Pressure. By correcting for the high-density vacuum of the early universe, we find that the cosmos is thermodynamically 2 trillion years old. This paradigm shift eliminates the need for "fast-track" galaxy formation theories and provides ample chronological space for the evolution of complex life and structure.

Acknowledgments

The author acknowledges the use of AI tools.

References

[1] P. A. M. Dirac, "The Cosmological Constants," *Nature*, 139, 323, 1937.

[2] D. W. Sciama, "On the Origin of Inertia," *MNRAS*, 113, 34, 1953.

[3] D. J. Schwarz et al., "Is the low-l microwave background cosmic?," *Phys. Rev. Lett.*, 93, 221301, 2004.

[4] K. Land and J. Magueijo, "The axis of evil," *Phys. Rev. Lett.*, 95, 071301, 2005.

[5] Y. Couder and E. Fort, "Single-particle diffraction," *Nature*, 444, 811, 2006.

[6] J. K. Webb et al., "Spatial Variation of Fine Structure Constant," *Phys. Rev. Lett.*, 107, 191101, 2011.

[7] Keenan, R. C., et al. "Evidence for a 300 Mpc scale under-density in the local galaxy distribution." The Astrophysical Journal 775.1 (2013): 62.

[8] Kovács, A., et al. "The integrated Sachs-Wolfe imprint of cosmic superstructures." MNRAS 451.4 (2015): 4236-4252.

[9] A. G. Riess et al., "Large Magellanic Cloud Cepheid Standards," *ApJ*, 876, 85, 2019.

[10] Y. Minami and E. Komatsu, "New Extraction of the Cosmic Birefringence from the Planck 2018 Polarization Data," *Phys. Rev. Lett.*, 125, 221301, 2020.

[11] C. Chang et al., "Dark Energy Survey Year 3," *Phys. Rev. D*, 107, 023530, 2023.

[12] D. Farrah et al., "Observational Evidence for Cosmological Coupling of Black Holes," *Astrophys. J. Lett.*, 944, L31, 2023.

[13] I. Labbé et al., "A population of red candidate massive galaxies," *Nature*, 616, 266, 2023.

[14] B. B. Kulangiev, "The Relativistic Walker: A Unified Hydrodynamic Field Theory of Matter, Vacuum, and Cosmos," *ResearchHub*, 2025. `https://www.researchhub.com/paper/10607672/the-relativistic-walker-a-unified-hydrodynamic-field-theory-of-matter-vacuum-and-cosmos`